

The influence of the lubricant from a rectilinear pair above the work accuracy of the elastic elements from the high precision mechanisms

MADALINA CALBUREANU
Faculty of Mechanics, University of Craiova
25 Nicolae Titulescu St., G2, 1fl, 5, 200219,
Craiova, ROMANIA
madalina.calbureanu@gmail.com

RALUCA MALCIU
Faculty of Mechanics, University of Craiova
Doljului St. C8c, 19
Craiova, ROMANIA
rmlciu@yahoo.com

MIHAI LUNGU
Faculty of Electrotechnics
University of Craiova
105-107 Decebal St. Craiova, ROMANIA
lma1312@yahoo.com

DAN CALBUREANU
University of Craiova
25 Nicolae Titulescu St., G2, 1fl, 5, 200219,
Craiova, ROMANIA
dan.calbureanu@gmail.com

Abstract: - The paper presents the determination by experiment of the vibration of a long elastic cinematic element with a mobile rectilinear pair, lubricated by two kinds of oil with low and high values for lubrication properties and cinematic viscosity. The lubricant pressures' field is analyzed by using the finite element method (COSMOSM program), starting with the datum obtained by experiment in the analysis of the elastic cinematic element vibration. The vibration acceleration for the elastic element was measured and the spectrum analysis was attached for each case separately. The efficacy acceleration and the power spectral density for different kinds of oil were comparatively presented. More actions are proposed for the high accuracy mechanism in order to obtain less vibration on the elastic cinematic elements.

Key-Words: - Lubricated rectilinear pair, elastic element, pressures field, film breaking phenomenon, spectral analysis

1 Introduction

As a result of several stringent requirements concerning higher work speeds and position accuracy of some points of the cinematic elements, it is more necessary to take into consideration the influence of the lubricant from the cinematic pairs. The pressure fields from the lubricant have a big influence over the vibrations that occur during the motion.

This work tries to prevent and control the apparition of the lubricant film-breaking phenomenon, which has consequences in the gripping and the working accuracy for the high precision mechanisms, especially for the robotic parts.

2 Problem Formulation

The considered mechanism is a slider-crank and connecting-rod assembly presented in figure 1. The vibrations of one long elastic element subjected to various spin speed of the leading element are experimentally measured. The rectilinear pair on the elastic element is lubricated with two kinds of oil.

Previously, the solving of the motion's equations of the elastic cinematic elements was made by assumption that these are continuous medium with infinite degrees of freedom, or they are discrete systems (using finite element method), or using the Lagrange's method from elastic-dynamics [4], [11]. This paper solves the equations of motion using Hamilton's principle and combines it with the Reynolds's lubrication equation [10].

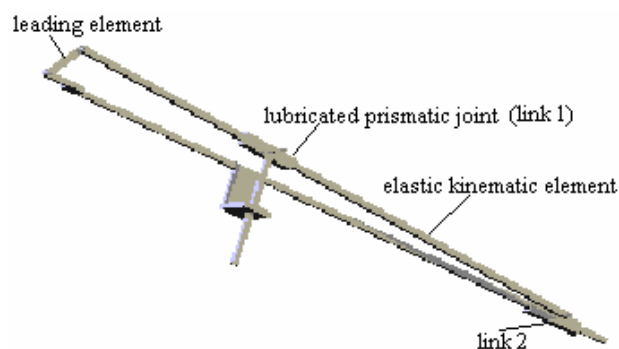


Fig. 1 The slider-crank and connecting-rod assembly

A crank and connecting-rod assembly with slide-bar is considered with rigid cinematic elements, excepting the 1m length element. A lubricated rectilinear pair with 0.100m length slides on this element.

Figure 2 shows the elastic cinematic element with the rectilinear pair.

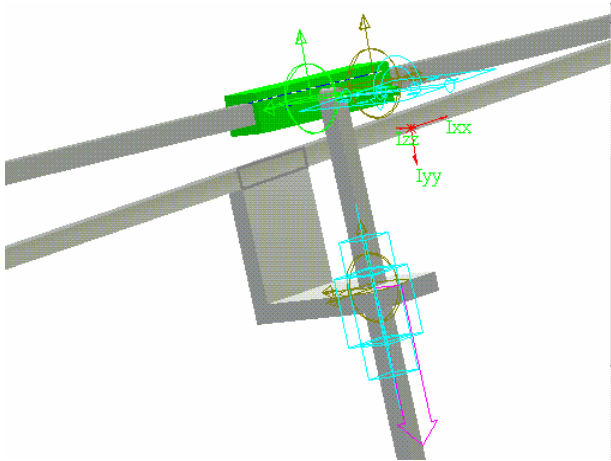


Fig. 2 Elastic cinematic element with mobile rectilinear pair and vertical element technologically loaded.

3 Algorithm, equations of motion and equation of the pressure field

The long cinematic element with the rectilinear pair slides on is considered linear elastic, with plane motion [2]. The equations of motion are obtained by using Hamilton's Principle from elastic-dynamics. The cinematic energy used in applying this principle is given by generalized speeds field theory used for elastic bodies.

This fact supposes the directly inclusion of inertial terms in the equations of motion [3]. The pressures distribution is computed by using Reynolds equations of lubrication for a viscous and incompressible fluid. An averaging on the transverse direction (z) is applied to this fluid and it is computed depending on the external force practiced on the cinematic element by the fluid [10]:

$$\xi^3 \frac{\partial^2 P}{\partial X^2} + 3\xi^2 \frac{\partial \xi}{\partial X} \frac{\partial P}{\partial X} = 6\mu V_r(t) \frac{\partial \xi}{\partial X}, \quad (1)$$

where: P is the distributed pressure from the film, $v_r(t)$ is the relative speed between the elastic element and the mobile rectilinear pair, ξ is the width of the film, μ is the dynamic viscosity of the film.

Moreover, it is verified the next relation by using geometry:

$$\xi = \frac{H}{2} - u_2(x^* + X, t). \quad (2)$$

The boundary conditions for $p(X, t)$ are given as:

$$X = 0 \Rightarrow P(0, t) = p_{atm}; \quad X = l \Rightarrow P(l, t) = p_{atm},$$

where p is the atmospheric pressure.

The general solution for the equation (1) is:

$$P(X, t) = 6\mu V_r(t) I_1(X, t) + C I_2(X, t) + C_1, \quad (3)$$

where:

$$I_1(X, t) = \int \frac{dX}{\left[\frac{H}{2} - u_2(X + x^*) \right]^2} \quad (4)$$

$$I_2(X, t) = \int \frac{dX}{\left[\frac{H}{2} - u_2(X + x^*) \right]^3}. \quad (5)$$

The constants C and C1 can be computed from the boundary conditions.

The integrals I1 and I2 are computed by using Fourier Transform method and the following values for them at the "n" iteration are obtained:

$$\begin{aligned} I_1^{(n)} &= -\frac{1}{n\pi} (H\gamma_3 - \gamma_4) \\ I_2^{(n)} &= -\frac{1}{n\pi} \left\{ \gamma_3 \left[\frac{H^2}{2} + \Phi^2(n, t) \right] + \left[\frac{1}{\gamma_2} + \frac{3H}{2\gamma_1} \right] \right\} \\ \gamma_1 &= \frac{H^2}{4} - \Phi^2(n, t) \\ \gamma_2 &= -\frac{H}{2} + \Phi(n, t) \sin\left(\frac{n\pi}{l} x\right) \\ \gamma_3 &= \gamma_1^{-3/2} \tan^{-1} \left[\frac{\Phi(l, t) - \frac{H}{2} \tan\left(\frac{n\pi}{l} x\right)}{\sqrt{\gamma_1}} \right] \\ \gamma_4 &= \frac{\Phi(n, t)}{2\gamma_1\gamma_2} \cos\left(\frac{n\pi}{l} x\right) \\ \Phi(n, t) &= \frac{2}{l} u_2^*(n, t) \end{aligned} \quad (6)$$

The sinus finite Fourier Transform of the force on the unit of length can be written as follows:

$$\begin{aligned} P^*(u_2^*(n, t), n, t) &= \\ &= B \int_{x^*}^{x^*+l} [6\mu V_r(t) I_1^{(n)} + C I_2^{(n)} + C_1] \sin(\beta_n x) dx \end{aligned} \quad (7)$$

Film breaking phenomenon occurs when the pressure computed with equation (3) decreases below the ambient pressure. In this case, Reynolds equation can't be applied inside the lubricant region [7].

The film breaking phenomenon occurring position can be established by changing the boundary

conditions (the pressures curve is easily translated in the film breaking phenomenon region)[8].

The boundary conditions are:

$$X = 0 \Rightarrow P(0, t) = p_{atm};$$

$$P(\bar{X}, t) = p_{atm} \quad \text{and} \quad \left. \frac{\partial p}{\partial X} \right|_{X=\bar{X}} = 0 \quad (8)$$

where: X is the position of the point where film breaking phenomenon occurs.

In order to obtain the numerical solution for the nonlinear differential equation from above there is used an algorithm with adaptive control for adjusting the step. Also, it is performed the numerical integration of the equation (6) for precise values for the time "t" and the $u_2^*(n, t)$. This is realized with one algorithm based upon the trapezes rule with automatically adjustment for the step for high accuracy.

The final solution for equation of movement it is obtained through inverting the sinus finite Fourier Transform and the applying the superposition principle:

$$u_2(x, t) = \sum_{n=1}^{n=\infty} \Phi(n, t) \sin(\beta_n x) \quad (9)$$

The rectilinear pair is lubricated by two kinds of oils with low and high lubricating properties as cinematic viscosity; its specific characteristics are shown in table 1.

Table 1 The characteristics of the types of oil used as lubricants in the rectilinear pair

Type of oil	Density [kg/m ³]	Dynamic Viscosity [Pa.s]
TB32E without additives STAS 742/81	890	0.02848
SHELL TONNA T STAS 871/68	894	0.19668

4 The mechanism modeling by SOLIDWORKS program – DYNAMIC DESIGNER modulus

As figure 1 shows us, the elements of the mechanism are as follows:

- the leading element;
- the long elastic cinematic element;
- the vertical technological element;
- the lubricated pair (1);
- the translational pair (2);
- the frame structure.

The cinematic elements of the mechanisms are made of steel ($\rho=7650 \text{ kg/m}^3$, $E= 207E9 \text{ N/m}^2$), having the lengths: $OA=0.07\text{m}$, $OC=1\text{m}$, bars with square sections $(0.011*0.011) [\text{m}^2]$.

Next step consists of introducing the necessary data for DYNAMIC DESIGNER program in order to realize the cinematic and dynamic analysis of the mechanism.

It is chosen the kind of movement for the leading element, the angular speed in our case.

The program offers the possibility of introducing in any kind of pair of the mechanism the mathematical equations which govern the movement of the elements.

The figure 3 presents the way of definition of the movement at the leading element.

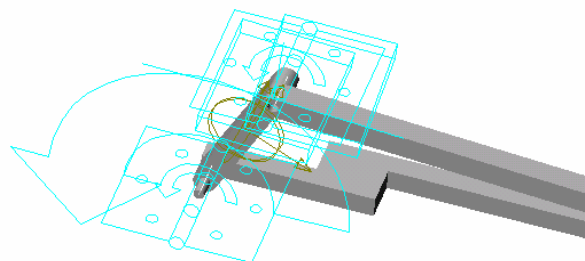


Fig. 3 The leading element movement way of definition

Figure 4 and figure 5 presents the technological force for the vertical element and the technological force for the translational pair 2 as vectors.

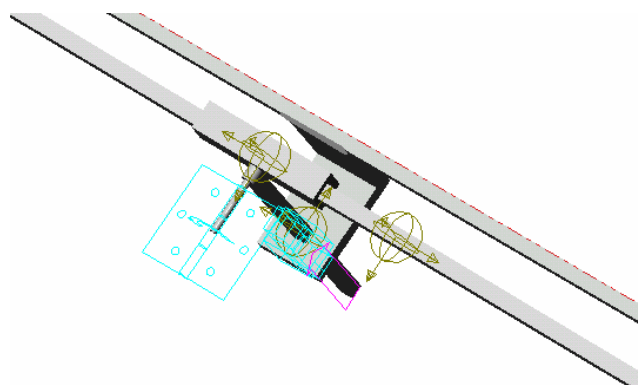


Fig. 4 The technological force at the vertical element

Then the program starts the movement simulation and data calculus for the cinematic and dynamic analysis.

The necessary data for the study of the lubricated pair 1 are:

- The cinematic analysis of the mechanism in order to determine the input data for the movement equation of the elastic element;

- The reaction force from the lubricated pair 1 – the R reaction force as input data in the movement equation of the elastic element;
- The relative speed pair- elastic element which is necessary for the finite element method calculus of the pressure field from the lubricant.

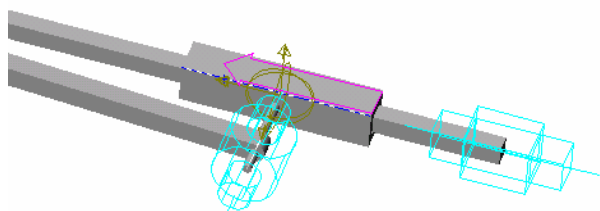


Fig. 5 The technological force at the translational pair 2

The cinematic analysis of the element is realized using the hypothesis of the constant angular speed at the leading element. The reactions and the torques can be computed for any pair of the mechanism on X, Y, Z directions as well the speeds and the accelerations of the mass centers of the elements, the angular speeds and accelerations for any elements. All these graphics are exported in the Excel program.

Table 2 presents the reaction values in the lubricated pair 1 in order to introduce them at the first step of the MAPLE program.

Table 2 The reaction values in the lubricated pair

Rotation [rpm]	120	200	300	387
Reaction [N]	2.91	7.867	18.03	29.18

5 Algorithm for the MAPLE program

The solving algorithm steps are as follows:

- the cinematic and kinetics-static analysis of the mechanism is made considering the hypothesis of the rigidity of all its cinematic elements;
- the equations of motion are solved by introducing an external force $R/(B*L)$ on the region occupied by the rectilinear pair and then, the pressures field is determined in the first approximation $p_1(X, t)$ [6];
- the distributed force $p_1(X, t)/B$, where B is the rectilinear pair width, is introduced in the new external force; then the equations of motion are solved again and so it is determined the pressures field in the second approximation.

This proceeding may continue by successively improving the mechanism dynamic reply, depending on the wished accuracy of the calculus [5].

It was achieved a MAPLE Program for computing this algorithm and it was determined the necessary datum by two iterations, with enough accuracy, compared afterwards with the experimental datum.

An important average used for simplifying the program was no considering the pressures field depending on time after the first iteration, but considering its effective value. Otherwise the model is difficult and it couldn't be solved anymore [1].

Furthermore, the pressure field from the rectilinear pair was modeled by finite element method with COSMOSM program. The specific heights of the oil film to the entrance and the exit of the pair were taken from the theoretical results of the deformations after the MAPLE program calculation of the deformations field.

6 Problem Solution

6.1 The theoretical results

The theoretical results for the deformation field are presented in figure 6 for the inferior oil in condition of the speed of 387 rpm at the leading element; figure 7 presents the same values but for the superior oil in the same work conditions.

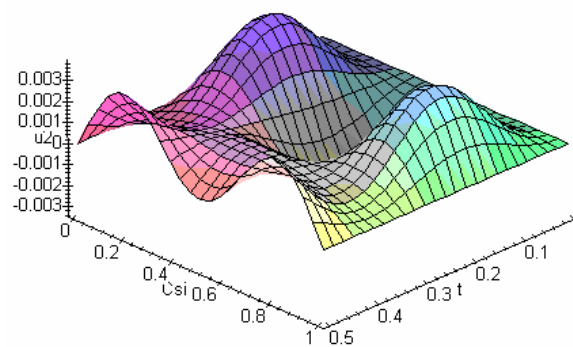


Fig. 6 The deformations field for the 387 rpm inferior oil

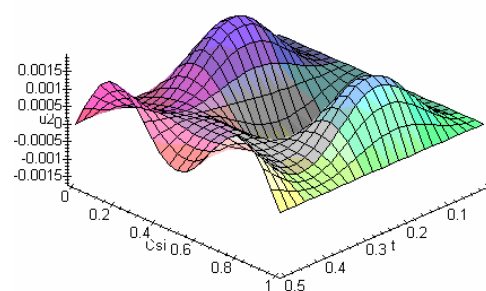


Fig. 7 The deformations field for the 387 rpm superior oil

The theoretical pressure fields computed by the mathematical model for the two types of oil and the 387 rpm are represented in figure 8, respectively 9. The maximal distributed pressure is $p= 0.016 \text{ N/m}$, reading the pressures map for rotation value 387 rpm, at the moment $t=0.0625 \text{ s}$ and $x= 0.1\text{m}$ for the inferior oil, and the maximal distributed pressure is $p=0.11\text{N/m}$ for 387 rpm rotation value at the moment $t=0.0379\text{s}$ and $x=0.1\text{m}$ for the inferior oil.

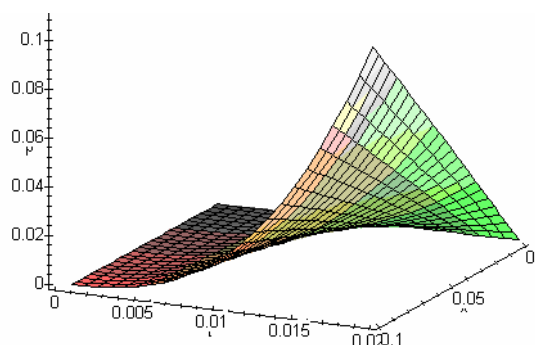


Fig. 8 Pressures field in lubricant at 387 rpm - superior oil

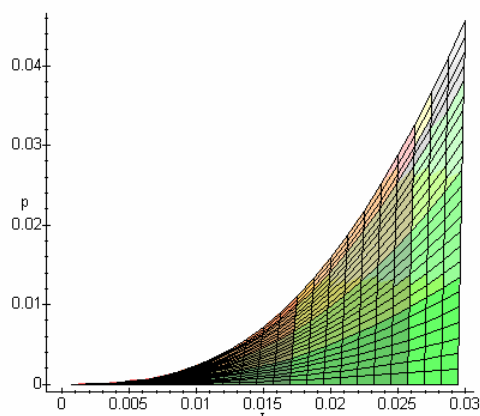


Fig. 9 Pressures field in lubricant at 387 rpm - inferior oil

6.2 The experimental results

The experimental results using the accelerometer device give the effective values of the vibration acceleration and the spectral analysis for every kind of oil and different rotation speeds of the leading element.



Fig. 10 The experimental device with all its components

The figure 10 presents all the components of the experimental device – the accelerometer, the computer interface, the mechanism, the engine.

The figure 11 presents the film breaking phenomenon for the inferior oil and the maximum rotation speed at the leading element on the long elastic element through the apparition of the longitudinal lines of gripping.

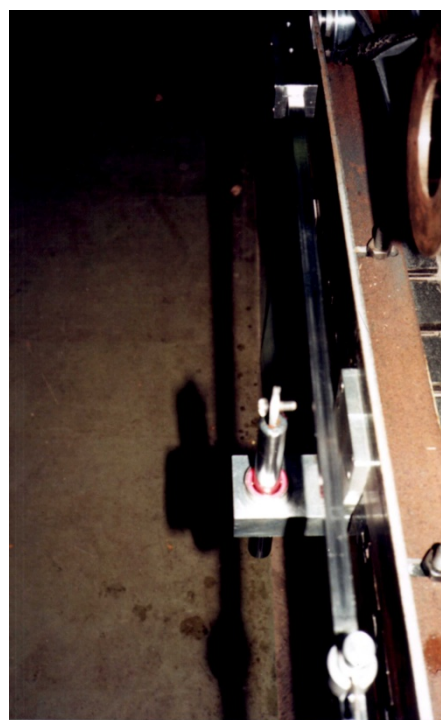


Fig. 11 The film breaking phenomenon for the inferior oil and maximum speed rotation at the leading element

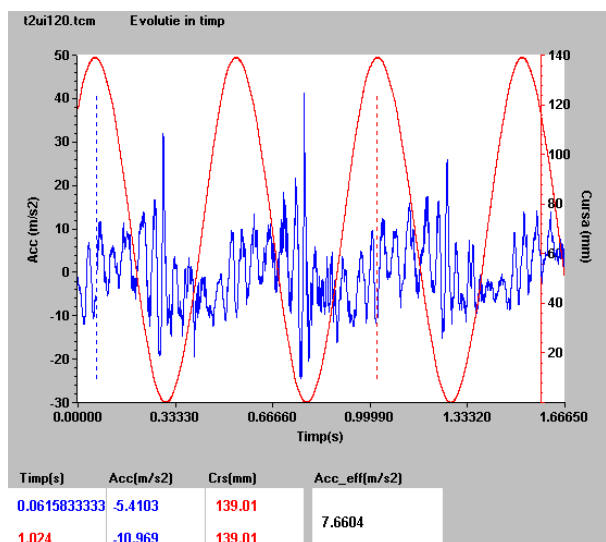


Fig. 12 The vibration acceleration for the inferior oil at 120 rpm

Figure 12 presents the experimental determinations for the inferior oil at 120 rpm. The effective value of the vibration acceleration is 7.66 m/s^2 .

Figure 13 presents the spectral analysis for the elastic element with inferior oil lubricated pair 1 in the same conditions.

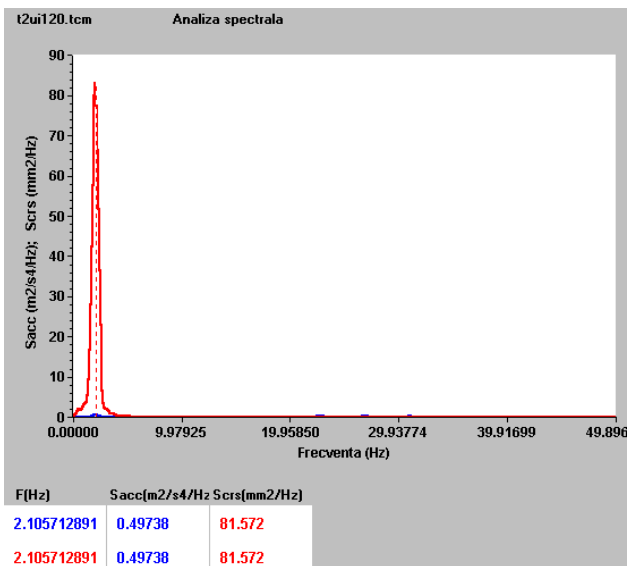


Fig. 13 The spectral analysis for the inferior oil at 120 rpm

Figure 14 presents the experimental determinations for the inferior oil at 387 rpm. The effective value of the vibration acceleration is 106.56 m/s^2 .

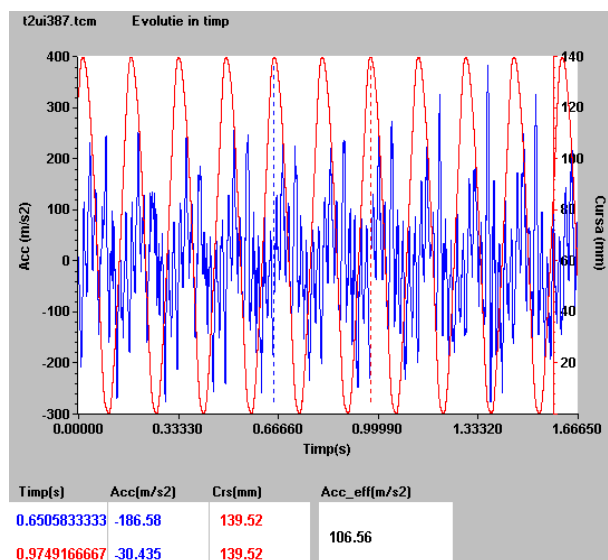


Fig. 14 The vibration acceleration for the inferior oil at 387 rpm

Figure 15 presents the spectral analysis for the elastic element with inferior oil lubricated pair 1 in the same conditions.

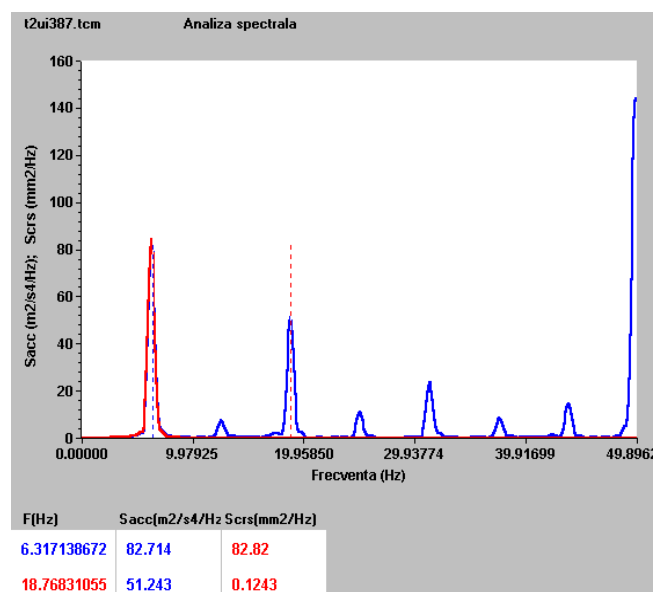


Fig. 15 The spectral analysis for the inferior oil at 387 rpm

Figure 16 presents the experimental determinations for the superior oil at 120 rpm. The effective value of the vibration acceleration is 5.5977 m/s^2 .

Figure 17 presents the spectral analysis for the elastic element with superior oil lubricated pair 1 in the same conditions.

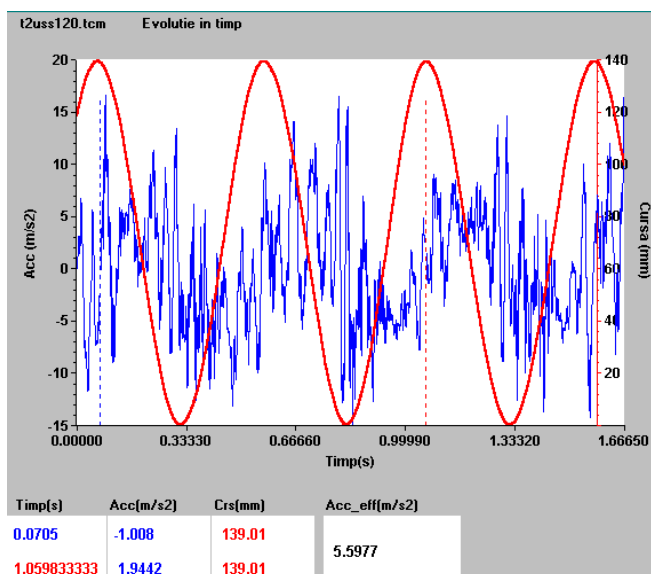


Fig. 16 The vibration acceleration for the superior oil at 120 rpm

The values of the vibration acceleration for the experimental determinations were compared with the values of the theoretical values obtained by the MAPLE program after the deformations field determination.

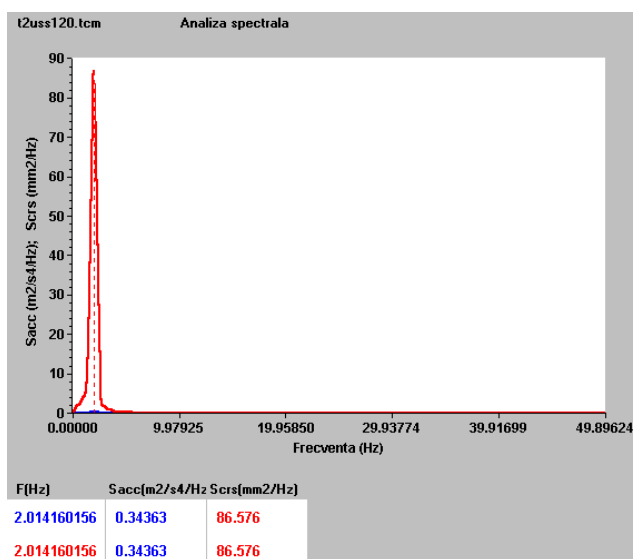


Fig. 17 The spectral analysis for the superior oil at 120 rpm

Figure 18 presents the experimental determinations for the superior oil at 387 rpm. The effective value of the vibration acceleration is 80.371 m/s².

Figure 19 presents the spectral analysis for the elastic element with superior oil lubricated pair 1 in the same conditions.

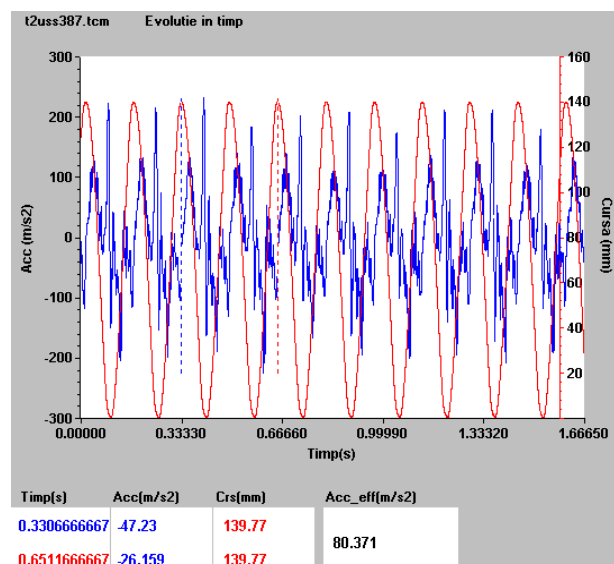


Fig. 18 The vibration acceleration for the superior oil at 387 rpm

The experimental results were compared to the ones given by the mathematical model solving. The compared characteristic quantity is the vibration acceleration and its values are shown in Table 3 for the inferior oil (TB32E).

The compared characteristic quantity is the vibration acceleration and its values are shown in Table 4 for the superior oil (SHELL TONNA T).

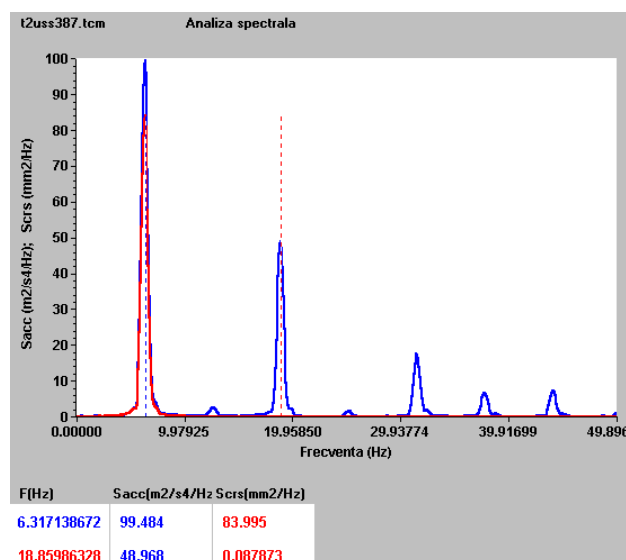


Fig. 19 The spectral analysis for the superior oil at 387 rpm

Table 3 Comparison between the theoretical vibration acceleration for the inferior oil at 387 rpm

Rotation [rpm]	120	200	300	387
----------------	-----	-----	-----	-----

Theoretical Vibration Acceleration [m/s ²]	7.23	13.47	62.41	106.06
Experimental Vibration Acceleration [m/s ²]	7.66	13.301	63.61	106.56

Type of the lubricant	Rotation [rpm]	H ₁ [mm]	H ₂ [mm]
Inferior	120	0.005323	0.00432
	200	0.005383	0.00473
	300	0.00538	0.00472
	387	0.005379	0.004713
Superior	120	0.005388	0.0047576
	200	0.005382	0.004728
	300	0.005387	0.004717
	387	0.0053788	0.0047093

Table 4 Comparison between the theoretical vibration acceleration for the superior oil at 387 rpm

Rotation [rpm]	120	200	300	387
Theoretical Vibration Acceleration [m/s ²]	5.39	12.41	51.06	79.43
Experimental Vibration Acceleration [m/s ²]	5.59	12.732	51.44	80.37

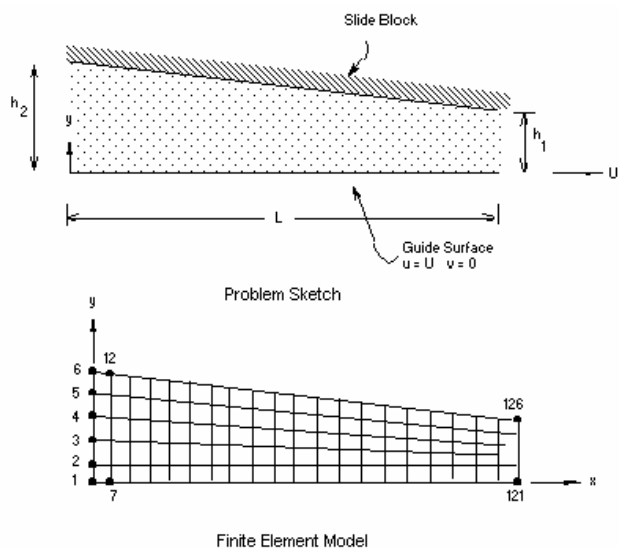


Fig. 20 The model with finite elements for the lubricant in the rectilinear pair

The lubricant film thicknesses at the entrance, respectively at the exit of the rectilinear pair, are computed with the datum obtained by solving the mathematical model.

Table 5 The h₁ and h₂ thicknesses of the lubricant

It was achieved a finite element routine COSMOS with this datum, considering the lubricant film as a plane laminar boundary layer [5].

Figure 21 presents the pressure field map in the lubricant for the inferior oil for the maximum rotation speed at the leading element.

Figure 22 presents the pressure field map in the lubricant for the superior oil for the maximum rotation speed at the leading element.

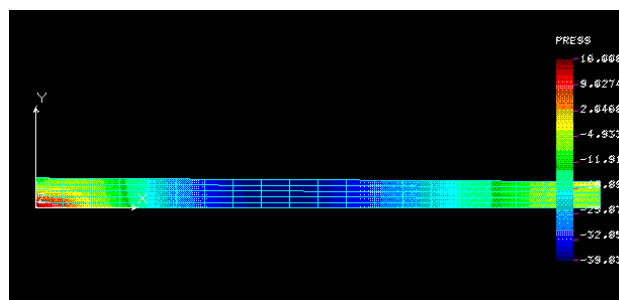


Fig. 21 Pressures distribution in inferior lubricant for 387 rpm rotation value

In figure 21 it can be noticed that the pressure value decreases below 0; this means that film breaking phenomenon appears.

The comparison between the theoretical and experimental results for the values of the pressures field is revealed in the table 6.

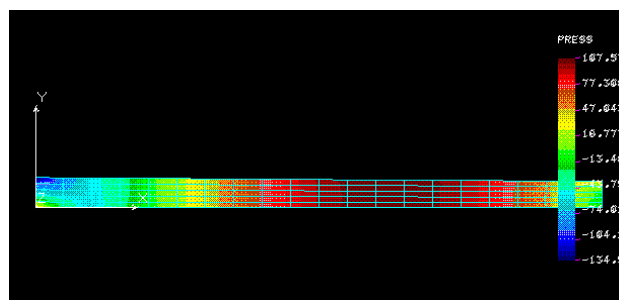


Fig. 22 Pressures distribution in superior lubricant for 387 rpm rotation value

Table 6 The comparison between the theoretical and experimental results for the values of the pressures field

Type of the lubricant N=387 rpm	Theoretical value for the pressure in lubricant [N/m ²]	The COSMOSM value for the pressure in lubricant [N/m ²]
Inferior	0.0160	0.016008
Superior	0.1100	0.10757

Table 7 The experimental values for the vibration acceleration [m/s²] for three kinds of oils and different rotations

Rotation [rpm]	120	200	300	387
Inferior oil	7.66	13.301	63.61	106.56
Medium oil	6.38	13.144	53.7	86.34
Superior oil	5.59	12.732	51.44	80.37

7 Conclusion

The influence of the lubricant from the rectilinear pair on the elastic cinematic element vibration was determined in the experimental way: the vibration amplitude varied from 0.005 m to 0.006 m for the oil with inferior characteristics and made decreasing mechanism working accuracy.

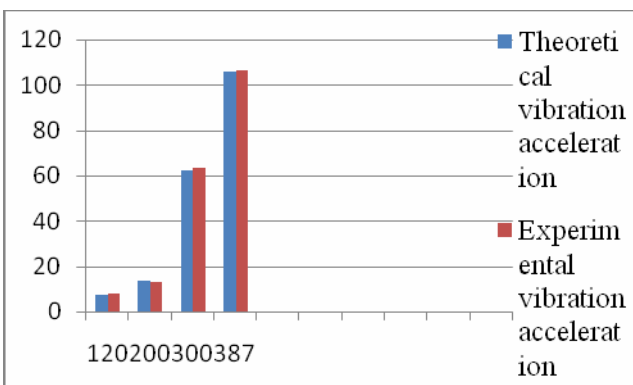


Fig. 25 The comparison between the theoretical and the experimental vibration acceleration [m/s²] for the

inferior oil (TB 32E) function of the rotation speed of the leading element

The vibration amplitude varied from 0.0019 m to 0.003 m for the superior oil and the film breaking phenomenon didn't appear for the used range of speeds.

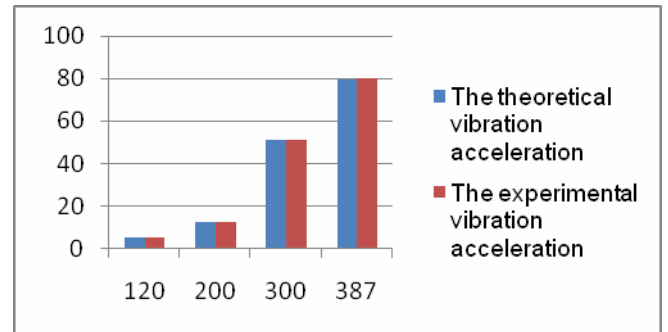


Fig. 26 The comparison between the theoretical and the experimental vibration acceleration [m/s²] for the superior oil (SHELL TONNA T) function of the rotation speed of the leading element

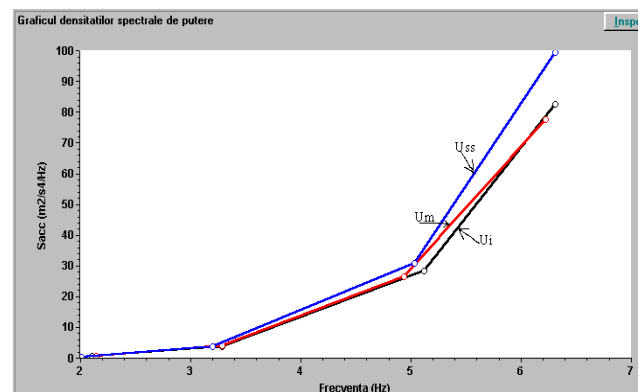


Fig. 23 The comparison between the effective values of the vibration acceleration for three kinds of oils

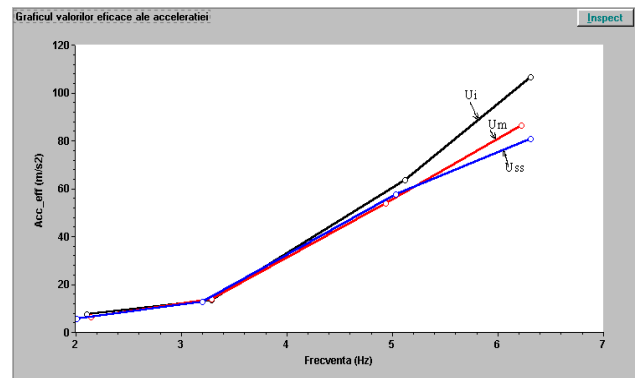


Fig. 24 The comparison for the power spectral densities for three kinds of oils

In the same time, the differences between the types of oil are low when the speed is low. When the speed of the leader element is high, the differences become higher.

The behavior of the mechanism and its precision in work is so better so the oil is better as quality: the properties of lubrication and viscosity.

The same situation is obtained when the speed is low. Knowing all these characteristics the deterioration of the elements of the mechanism can be avoided.

Besides, lubricant film breaking phenomenon appeared in the pressure field from the lubricant film and they may bring about gripping and deteriorating the accuracy of mechanism's elements movements.

MAPLE routine has a great level of generality. It may be applied to any plane-moving element with a mobile lubricated rectilinear pair [9]. This routine computes the pressure field in lubricant and the maximal deformations of an elastic element with the accuracy less than 8%.

It may be used as entrance variable quantity: material properties of the elastic elements, its dimensions, the lubricant viscosity characteristics and the length of the rectilinear pair, as well as the driving element rotation.

The future directions of research include the material changing of the elastic element, using a larger and continuous interval for angular velocity on the leading element of mechanism for determination the exact moment of film breaking phenomenon appearance.

References:

- [1] Bognar, G., - *Numerical approximations of some nonlinear problems*, WSEAS Mathematics & Computers in Mechanical Engineering, MCME 2000, pp. 5351-5356
- [2] Brown, H. - *507 Mechanical Movements: Mechanisms and Devices*, Dover Publications (August 15, 2005)
- [3] Călbureanu, M., Malciu, R., Călbureanu, D., - *The Experimental Measurements Of The Vibrations For A Long Elastic Cinematic Element Influenced By The Operating Conditions And The Lubricant*

From The Mobile Rectilinear Pair, International Conference "Advanced Concepts in Mechanical Engineering" ACME IASI 2004; Buletinul Științific de Iași, pag. 107-112

[4] Eckhardt, H. - *Kinematic Design of Machines and Mechanisms*, McGraw-Hill Professional; 1 edition, 1998

[5] Erdman, J. Holte, T. Chase - *Approximate Velocities in Mixed Exact-Approximate Position Synthesis of Planar Mechanisms*, ASME Journal of Mechanical Design, Vol. 123, pp. 388-394, Sept. 2001.

[6] Jacobson, B. - *The film lubrication of real surfaces*, Tribology International, vol. 33, Elsevier Sciences Ltd., pp. 205-210, 2000

[7] Prudhoe, L, Venner, C.H., Caun, P.M. Spikes, H. - *Experimental and Theoretical Approaches to Thin Film Lubrication Problems*, IUTAM Symposium on Elasto-hydrodynamics and Microelasto-hydrodynamics, Cardiff, U.K., 2004

[8] Santos, I., Estupina, E., - *Combining Multibody Dynamics, Finite Elements Method and Fluid Film Lubrication to Describe Hermetic Compressor Dynamics*, 6th WSEAS International Conference on SYSTEM SCIENCE and SIMULATION in ENGINEERING, Venice, Italy, November 21-23, 2007, pp. 237

[9] Wang Z., Ji S., Wan Y., Sun J., Ou C., Pan Y. - *Kinematic Analysis and Dexterity of a New STPM* - Proceedings of the 7th WSEAS International Conference on Robotics, Control & Manufacturing Technology, Hangzhou, China, April 15-17, 2007, p. 316

[10] White, M. Fr. - *Viscous Fluid Flow*, McGraw Hill, 3 edition, 2005

Yang, Y, Zhao, B.G, Chen, J, Song, T. - *Modelling study on a forward recursive construction approach of dynamical equations of mechanism systems with flexible articulated joints*, 5th WSEAS Int. Conf. on ENVIRONMENT, ECOSYSTEMS and DEVELOPMENT, Tenerife, Spain, December 14-16, 2007, pp 103

[11] Zienkiewicz, O., C., Taylor, R.L., Nithiarasu P. - *The Finite Element Method for Fluid Dynamics*, Sixth Edition, McGraw Hill, 2005